



# Electromagnetic emission of integrated circuits induced by ionizing radiation and its measurement uncertainties

Nikolaus Czepl · Nikolaus Juch · Bernd Deutschmann

Received: 25 October 2023 / Accepted: 11 December 2023 / Published online: 17 January 2024  
© The Author(s) 2024

**Abstract** In this article, we show the change of electromagnetic emission (EME) of integrated circuits (ICs) and their external circuitry induced by the presence of ionizing radiation. We use the 150 Ohm method according to IEC 61967-4 to characterize the conducted emission of our tested integrated circuit (IC) at the VDD pin. Simultaneously to measuring the electromagnetic emission, we irradiate the IC with X-rays. The irradiation process is carried out up to a dose of 5 Mrad using a high-power X-ray radiation source. The electromagnetic emission spectra are retrieved before, during and after the irradiation process. We also show that special caution regarding radio frequency (RF) measurements must be used when performing combined testing. Therefore, we analyze the composition of measurement uncertainties of electromagnetic compatibility in combination with ionizing radiation hardness characterization. This article contains measurement results showing the negative impact of ionizing radiation on the electromagnetic compatibility (EMC) of an IC. Additionally we provide measures to ensure properly combined measurements of EME and ionizing radiation. Therefore we show how to reduce the electromagnetic interference originating from the high-voltage generator that is necessary to generate X-rays.

**Keywords** Electromagnetic Emission (EM) · Electromagnetic Compatibility (EMC) · Radiation hardness · Combined EMC testing · IEC 61967

## Elektromagnetische Störemission von integrierten Schaltkreisen verursacht durch ionisierende Strahlung sowie die Bestimmung der Messunsicherheiten

**Zusammenfassung** In diesem Artikel zeigen wir die Veränderung der elektromagnetischen Emission (EME) von integrierten Schaltkreisen (ICs) und der externen Beschaltung, die durch ionisierende Strahlung ausgelöst wird. Wir verwenden die 150 Ohm-Methode nach IEC 61967-4, um die leitungsgebundene Störemission unseres Test-ICs am VDD-Pin zu charakterisieren. Gleichzeitig mit der Messung der elektromagnetischen Emission bestrahlen wir den IC mit Röntgenstrahlen. Die Bestrahlung erfolgt bis zu einer Dosis von 5 Mrad mit einer Hochleistungs-Röntgenstrahlungsquelle. Die elektromagnetischen Emissionsspektren werden vor, während und nach dem Bestrahlungsprozess aufgenommen. Wir zeigen auch, dass bei der Durchführung von kombinierten Tests besondere Sorgfalt bei Hochfrequenzmessungen (RF) notwendig ist. Daher analysieren wir die Zusammensetzung der Messunsicherheiten der elektromagnetischen Verträglichkeit in Kombination mit der Strahlungsfestigkeitsmessung mit ionisierender Strahlung. Dieser Artikel enthält Messergebnisse, die den negativen Einfluss von ionisierender Strahlung auf die elektromagnetische Verträglichkeit (EMV) eines ICs zeigen. Darüber hinaus gehen wir auch auf Maßnahmen zur Sicherstellung korrekter kombinierter Messungen von EME und ionisierender Strahlung ein. Deshalb zeigen wir, wie man den Störeinfluss des Hochspannungsgenerators, der zur Erzeugung von Röntgenstrahlen erforderlich ist, minimiert.

N. Czepl (✉) · N. Juch · B. Deutschmann  
Institute of Electronics (IFE), Graz University of Technology,  
Inffeldgasse 12/I, 8010 Graz, Austria  
czepl@tugraz.at

**Schlüsselwörter** Elektromagnetische Emission (EME) · elektromagnetische Verträglichkeit (EMV) · Radiation hardness · Kombinierte EMV Prüfung · IEC 61967

## 1 Introduction

Integrated circuits (ICs) are indispensable components in almost all modern electronic systems. An integral aspect of designing ICs revolves around assessing their reliability and functionality throughout their lifespan. This is especially crucial in demanding environments like aerospace, avionics, or automotive applications. In such contexts, it becomes important to understand whether environmental factors such as ionizing radiation, transient disturbances, or radio frequency interference (RFI) cause any alterations in their internal behavior over time.

Typically, ICs emit a low level of electromagnetic radiation directly from their package since their internal dimensions are too small to serve as efficient transmitting antennas. Moreover, there are studies that demonstrate that the emission level is directly dependent on how signals and power supply are routed inside the chip [14]. However, they are often considered the source of radiated emissions from the entire electronic system due to their internal switching activity, which manifests as conducted emissions coupled out via the pins/balls of the IC package. Consequently, efforts are made to manage emission levels both internally and externally to ensure compliance with normative requirements for electromagnetic emissions. In this context, considerations of EMC of ICs play a pivotal role in the design process. However, there has been little research into whether EMC also changes with advancing age and the associated aging processes. For example, EMC tests are currently being performed on new, unaged, unirradiated assemblies.

So far, there is limited literature addressing this potential relationship. Some notable works in this field include those by Benfica et al. [3], Goerl et al. [10], and Czepl et al. [6], which investigated CMOS circuits for their electromagnetic compatibility under radiation exposure. Regarding aging effects, some research was done by Ghfiri [9], Benfica et al. [4] and Soares et al. [15], analysing the influence of aging, voltage over-stress and thermal over-stress on the EMC behaviour of ICs.

Significant research has gone into standardizing radiation hardness, leading to the introduction of various standards for characterizing semiconductor devices in terms of their behavior under ionizing radiation (e.g., ASTM F1892-12(2018) [8], MIL-STD-750-1, MIL-STD-883, ESA-ESCC-22900). Similarly, the EMC community has established several IC-level standards to characterize the electromagnetic emission and immunity of ICs (e.g., IEC 61967 [12] or IEC 62132[13]).

A common feature of all these standards is that they investigate behavior under specific operating condi-

tions, often under standard conditions. Typically, ICs are examined for their EMC behavior at room temperature ( $23 \pm 5$ )°C, with the ICs operating under nominal conditions, without considering additional environmental factors such as radiation that might cause single-event effects or stress-induced degradation like total ionizing dose (TID). Therefore, it becomes pertinent to explore the EMC behavior of a circuit after it has been exposed to an accelerated stress test equivalent to an expected dose (e.g., equivalent to 25 years of operation in a satellite in geostationary orbit). As emphasized in a publication from the Indian Space Agency [5], the received TID depends significantly on instrument shielding. Nonetheless, it is reasonable to anticipate doses of up to 50krad per year when designing electronic circuits for geostationary orbits, resulting in a TID exceeding 1 Mrad for satellite missions exceeding 20 years.

This paper's scientific investigations offer an overview of the feasibility and interactions of various established test methods from both fields – EMC and TID testing – when combined. These investigations aim to determine whether ionizing radiation stress affect the electromagnetic behavior of ICs. With this goal in mind, these investigations involve measurements of EMC behavior after different levels of TID stress.

Sect. 2 of this paper presents an outline of the measurement setup used in the experiment, while Sect. 3 provides the combined characterization results. Sect. 4 analyzes the measurement uncertainties of the EME measurements in this measurement setup. In the final section, the scientific findings are discussed, and prospects for further combined characterization experiments are outlined.

## 2 Measurement Setup for Combined Testing

### 2.1 Device under test (DUT)

The device utilized for the combined effects investigations described herein is a test chip meticulously designed and fabricated using a 0.35  $\mu\text{m}$  complementary metal oxide semiconductor (CMOS) process. The primary objective of this chip was to enhance the performance of CMOS output drivers in terms of their electromagnetic emission. To attain this goal, a weighted and distributed control mechanism was implemented for the output transistors to optimize the shape of the output waveform. This optimization was achieved by configuring different threshold voltage values within the pre-drivers responsible for generating the gate signals for the actual output transistors. For a more comprehensive understanding, please refer to the detailed explanation in [7]. For our investigations in this article we used three devices under test (DUTs) in total. DUT 1 is a test chip that includes 8 CMOS output buffers. It was irradiated up to 5Mrad with a dose rate of  $5\text{Mrad h}^{-1}$ . DUT 2 is the same device like

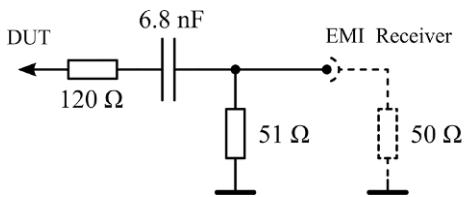


Fig. 1 150  $\Omega$  coupling network

DUT 1 and was irradiated up to 1.5 Mrad with a dose rate of  $1.5 \text{ Mrad h}^{-1}$ . DUT 3 is similar to DUT 1 but incorporates additionally on-chip decoupling capacitors. It was irradiated up to 1.5 Mrad with a dose rate of  $1.5 \text{ Mrad h}^{-1}$ .

## 2.2 Characterizing the conducted electromagnetic emission of an IC (150-Ohm method)

The IEC 61967-4 standard introduces the 150-Ohm method, which facilitates the measurement of RF voltage at IC pins within a frequency range spanning from 150 kHz to 1 GHz [12]. This characterization technique serves the purpose of determining the emission contribution of individual IC pins or groups of pins, and it is notable for its excellent repeatability in emission measurements. Typically, this method is employed solely for IC pins that are connected to a printed circuit board (PCB) trace exceeding 10 cm in length or directly linked to a cable.

In this procedure, the pertinent pins are loaded with a typical antenna impedance of 150  $\Omega$ . This is achieved using the coupling network illustrated in Fig. 1. The coupling network is then connected to a spectrum analyzer or electromagnetic interference (EMI) receiver, both of come with a typical input impedance of 50  $\Omega$ . The network is therefore designed as a 150  $\Omega$  to 50  $\Omega$  impedance matching network.

To characterize the impact of Ionizing radiation on the EME of the device under test (DUT), a test circuit is configured which is schematically represented in Fig. 2. All eight output buffers of the three test chips drive simultaneously a parallel ohmic and capacitive load, imitating a typical load case for a digital output driver, of 47 pF and 10 k $\Omega$ . The switching frequency is generated by an external crystal oscillator with a fre-

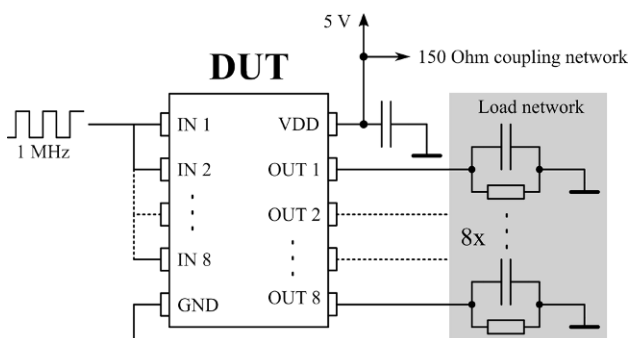


Fig. 2 Schematic representation of the utilized test circuit

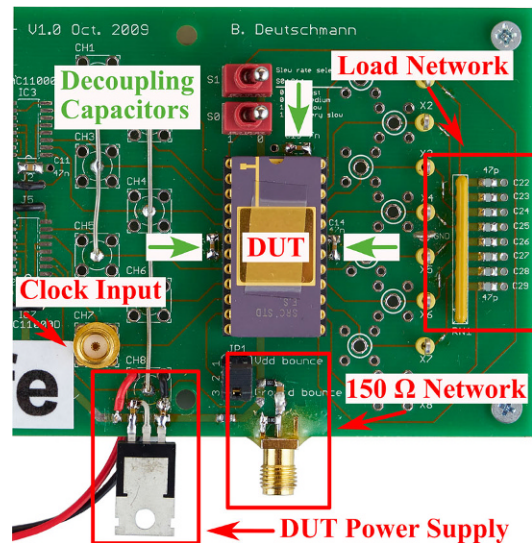
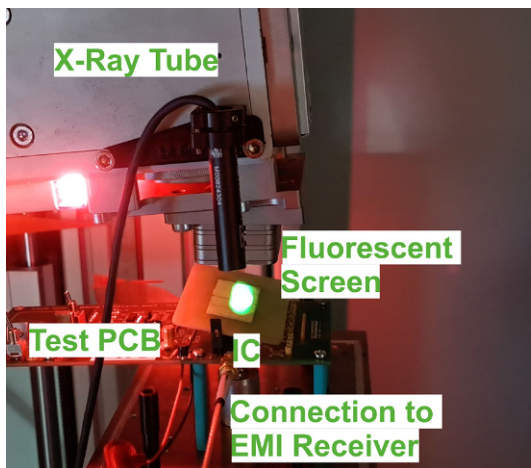


Fig. 3 Hardware implementation of the 150  $\Omega$  coupling network

quency of 1 MHz. To ensure proper operation, the IC is supplied with 5V via its three supply connections, each of which was equipped with a 47 nF X7R multi layer ceramic capacitor (MLCC) for decoupling purposes. We used 9V Batteries to power the circuit, as well as the oscillator, to avoid electromagnetic influence of the supply on the measurement results. The conducted EME at the VDD pin of the IC is measured using a 150  $\Omega$  coupling network connected to an EMI receiver.

The test circuit was implemented on a modified test PCB which is illustrated in Fig. 3. It shows the ohmic-capacitive load network, the 150  $\Omega$  network, the IC's power supply, clock input as well as the position of the decoupling capacitors. Special care was taken to limit the effects of EME originating from peripheral components, which would make it difficult to detect subtle X-ray-induced changes in the DUT's electromagnetic emission behavior. This was achieved, by providing the DUT with an individual linear voltage regulator while supplying the clock signal via an external, battery-powered clock generator. Doing so removes all peripheral circuits from the DUT's supply net, preventing them from generating additional EME. In addition, the clock signal itself was low pass filtered to attenuate unneeded harmonic contents. This limits the effect of capacitive coupling between the clock traces and the DUT's power supply, which otherwise causes a noticeable amount of EME, picked up by the 150  $\Omega$  network. In addition to all the measures on PCB-level, we also had to block common-mode disturbances at the coaxial cable induced by the high voltage generator by using several ferrite cores.



**Fig. 4** Test setup inside the irradiation chamber. At this stage, a fluorescent screen was placed on top of the DUT to verify the irradiated area

### 2.3 Irradiation of the DUT

Irradiation is carried out within an X-Ray cabinet using a tungsten-target X-Ray tube operating at an accelerating voltage of 40 kV. The dose rate is adjusted as a function of the cathode current. For a dosage rate of  $1.5 \text{ Mrad h}^{-1}$  a cathode current of 7 mA needs to be set, for  $5 \text{ Mrad h}^{-1}$  25 mA cathode current is used. To precisely determine the dose rate, a calibrated photodiode is utilized, yielding a photodiode current at a rate of  $417 \text{ rad s}^{-1} \text{ mA}^{-1}$ , which corresponds to an approximate dose of  $1.5 \text{ Mrad h}^{-1}$ . Consequently, the total irradiation duration is set to 1 hour to attain the desired cumulative dose of  $1.5 \text{ Mrad h}^{-1}$  and  $5 \text{ Mrad h}^{-1}$  respectively. Fig. 4 illustrates the actual irradiation setup inside the chamber. The fluorescent screen is used to determine the correct position of the X-Ray beam and is removed for the actual irradiation process. In order to bring the ionizing energy directly into the silicon, it is necessary that the die is exposed. Therefore, we use ceramic packages with removable lids for our DUTs.

Notably, the IC could remain within the irradiation chamber for the entire duration of the process, as the connecting cable to the EMI receiver could be threaded through the device. This approach is important in minimizing handling time and preventing the effects of annealing of radiation-induced defects influencing our measurements.

## 3 Measurement Results

This section provides an overview and explanation of the outcomes derived from EME measurements combined with the X-ray irradiation experiments.

### 3.1 Emission Spectra

The main results of these investigations are the emission spectra of the DUTs at the VDD supply pin. The first DUT DUT 1 is a slew rate controlled output buffer which is irradiated to a dose of 5 Mrad. At a dose rate of  $5 \text{ Mrad h}^{-1}$ , an emission spectrum is recorded every 6 min, resulting in dose steps of 500 krad. During the measurement of the emission spectrum, the irradiation has not been stopped, which is a great advantage of the chosen 150-Ohm method.

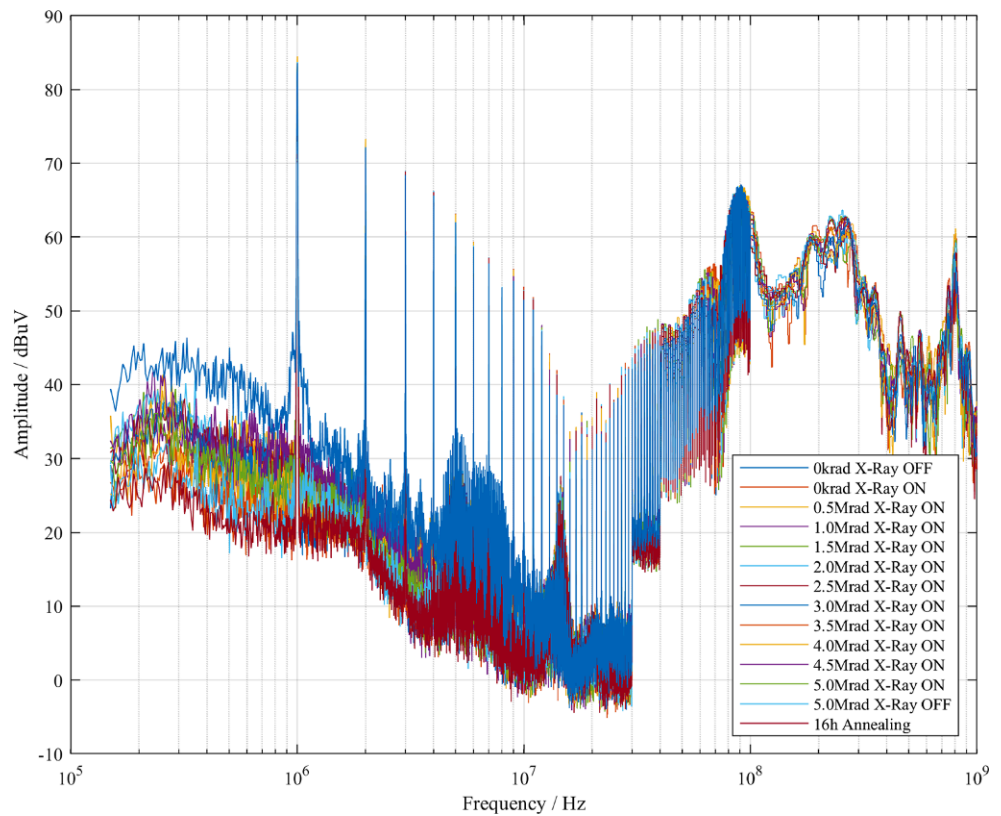
Fig. 5 shows the emission spectra of DUT 1 for a dose range of 0 Mrad to 5 Mrad including measurements before the start of the irradiation and after the radiation source is turned off. Additionally, we also measure the emission spectrum of the IC after 16 h annealing time, to take into account the reversible influence of the radiation as well.

Fig. 5 shows the fundamental frequency of the oscillator at 1 MHz and in addition all the harmonics of a trapezoidal signal. As our chosen duty cycle of the input signal is 20%, also even order harmonics are appearing in our emission spectrum. This emission spectrum also shows the effect of the used external decoupling capacitor, which is adding a notch to the emission spectrum. At approximately 20 MHz, the resonance frequency of the decoupling capacitor can be observed. In this frequency area, the largest change of the emission peaks in dependence of ionizing radiation is visible. In general, it can be seen that the noise floor between emission peaks varies greatly, up to 20 dB between measurements. In order to understand the precision of our measurements, we also perform a detailed analysis of the measurement uncertainty of the EMI receiver in Sect. 4.

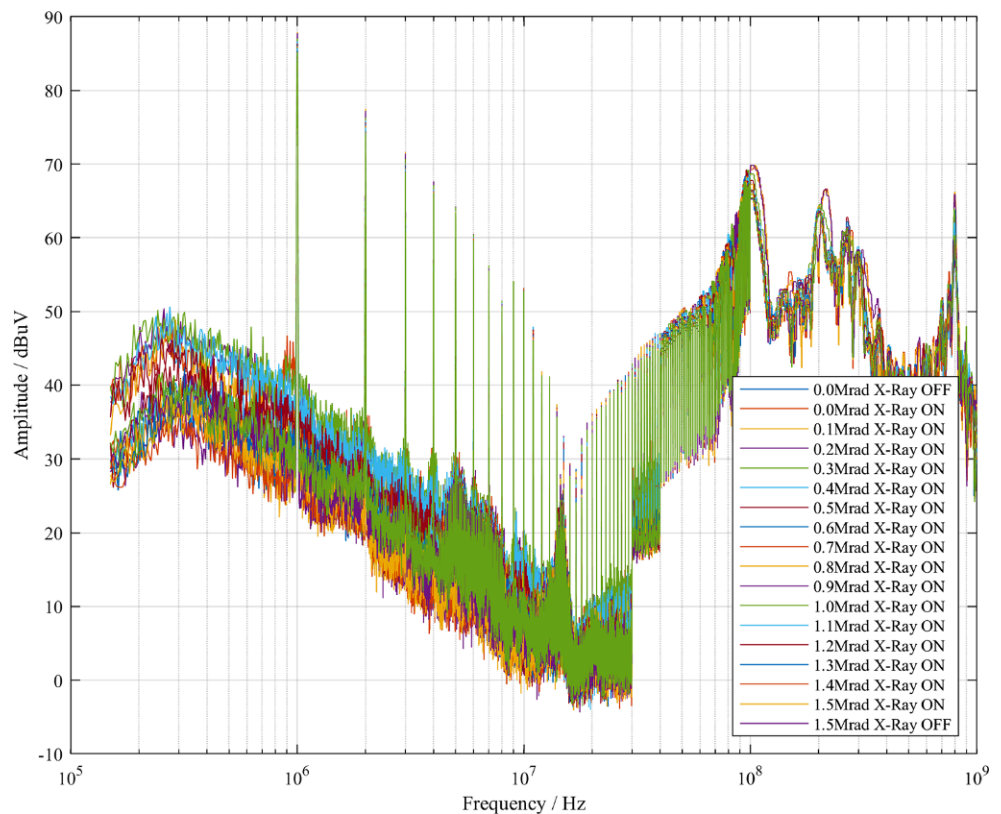
Fig. 6 shows the emission spectra of DUT 2 for a dose range of 0 Mrad to 1.5 Mrad including measurements before the start of the irradiation and after the radiation source was turned off. Based on Fig. 8, our thoughts were that up to 1.5 Mrad most of the changes in emission due to radiation can be seen. Therefore, the maximum dose for DUT 2 is reduced to 1.5 Mrad. Again, at approximately 20 MHz, the resonance frequency of the decoupling capacitor can be observed. Compared to DUT 1, the change of the emission peaks in dependence of ionizing radiation is less. However, again as with DUT 1, the largest changes in conducted emission are seen at the resonant frequency of the decoupling capacitor.

Fig. 7 shows the emission spectra of DUT 3 for a dose range of 0 Mrad to 1.5 Mrad including measurements before the start of the irradiation and after the radiation source was turned off. Again, the maximum dose for DUT 3 is set to 1.5 Mrad. DUT 3 generally shows less emissions than DUT 2 or DUT 1 because this IC has on-chip decoupling capacitors built in in addition to the slew rate controlled output buffers. With this technique, all free chip areas are filled with capacitors, which provide additional stabilization of

**Fig. 5** Emission spectra of DUT 1 for different irradiation doses. The plot also includes emission spectra with the shutter of the X-ray tube closed at the beginning of the irradiation process, and at the end of the irradiation process. In addition, the effect of annealing on the emission spectrum is investigated 16 h after the irradiation



**Fig. 6** Emission spectra of DUT 2 for different irradiation doses. The plot also includes emission spectra with the shutter of the X-ray tube closed at the beginning of the irradiation process, and at the end of the irradiation process



**Fig. 7** Emission spectra of DUT 3 for different irradiation doses. The plot also includes emission spectra with the shutter of the X-ray tube closed at the beginning of the irradiation process, and at the end of the irradiation process

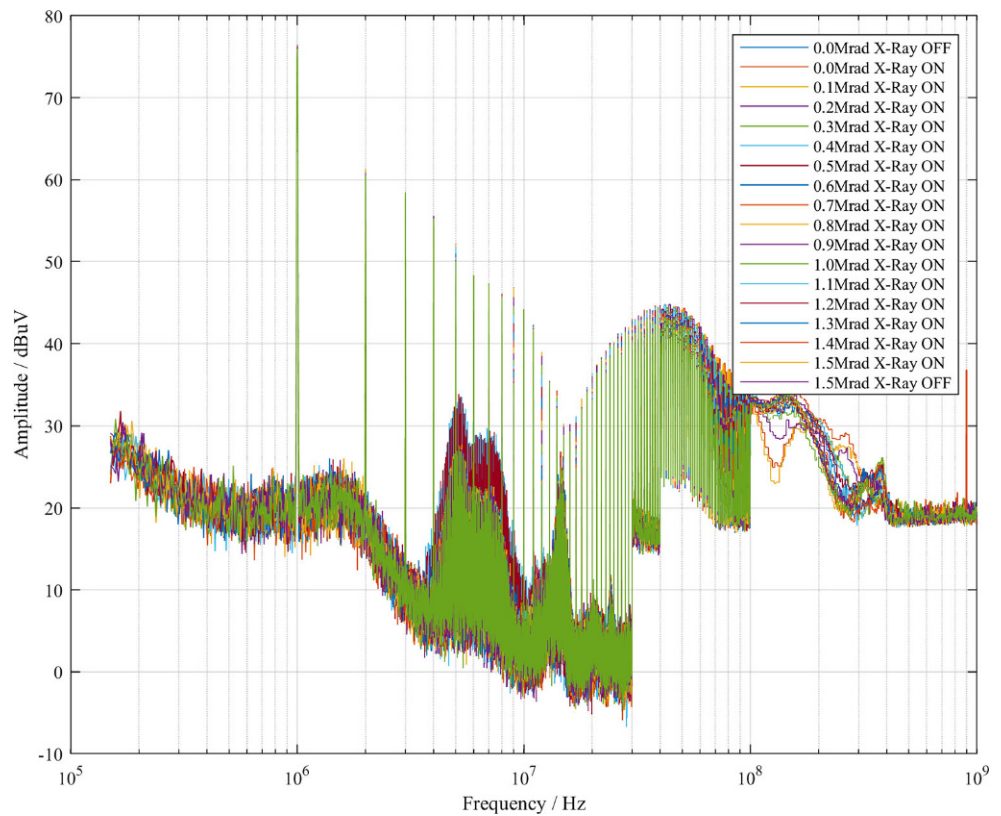
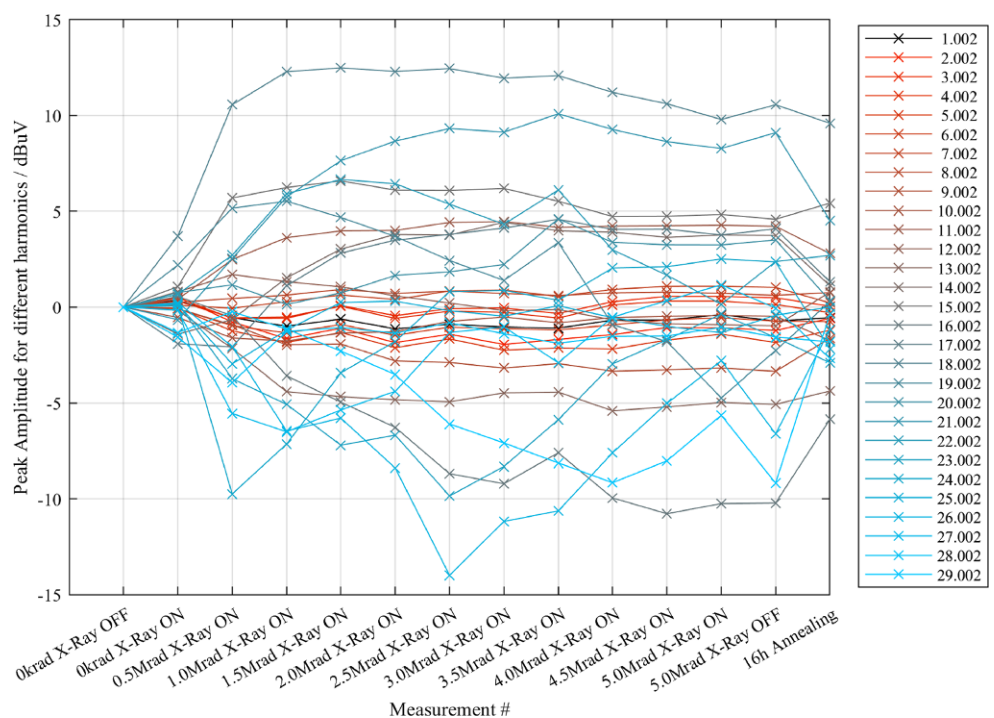


**Fig. 8** Behavior of the harmonics of the emission spectrum with increasing radiation dose of DUT 1. The black line indicates the fundamental frequency, the colored lines the respective harmonics (in MHz)



the supply voltage. Again, at approximately 20 MHz, the resonance frequency of the external decoupling capacitor can be observed. Compared to DUT 1, the change of the emission peaks in dependence of ionizing radiation is less. However, again as with DUT 1, the largest changes in conducted emission are visible

at the resonant frequency of the decoupling capacitor. Obviously, the irradiation is not really affecting the behaviour of the on-chip decoupling capacitors.

**Fig. 9** Behavior of the harmonics of the emission spectrum with increasing radiation dose of DUT 2. The black line indicates the fundamental frequency, the colored lines the respective harmonics (in MHz)

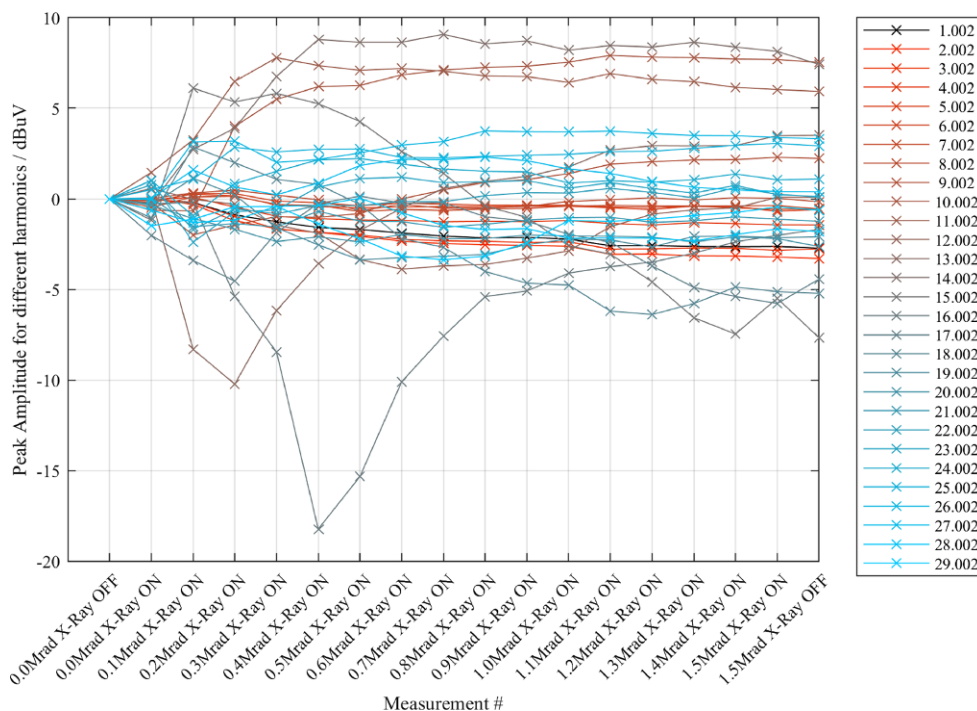
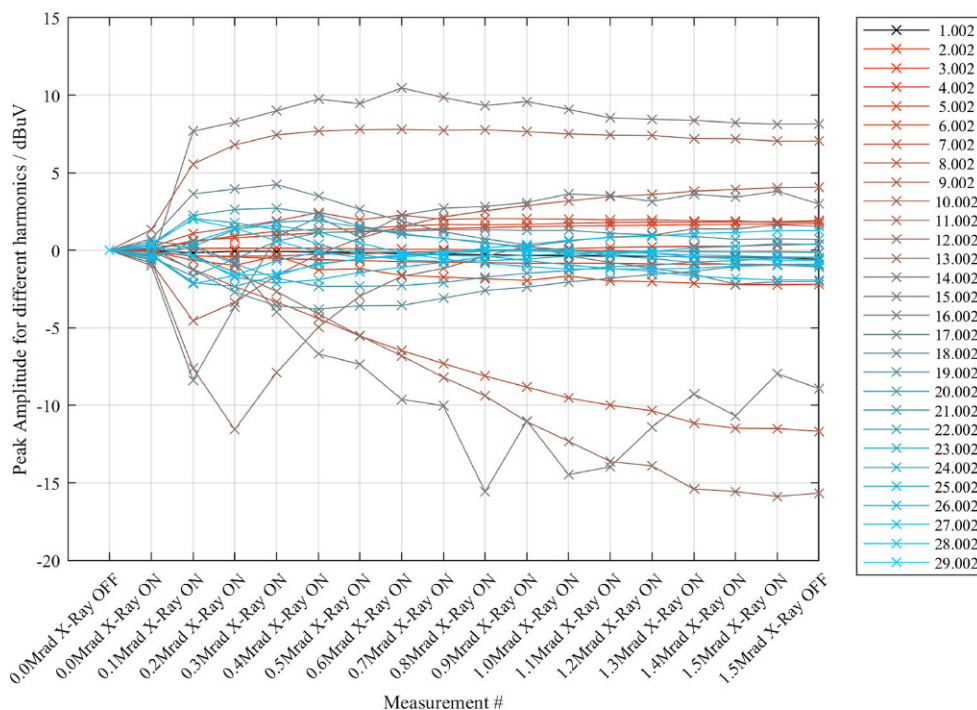


**Fig. 10** Behavior of the harmonics of the emission spectrum with increasing radiation dose of DUT 3. The black line indicates the fundamental frequency, the colored lines the respective harmonics (in MHz)



### 3.2 Investigation of harmonics below and above the resonance frequency of the decoupling capacitor

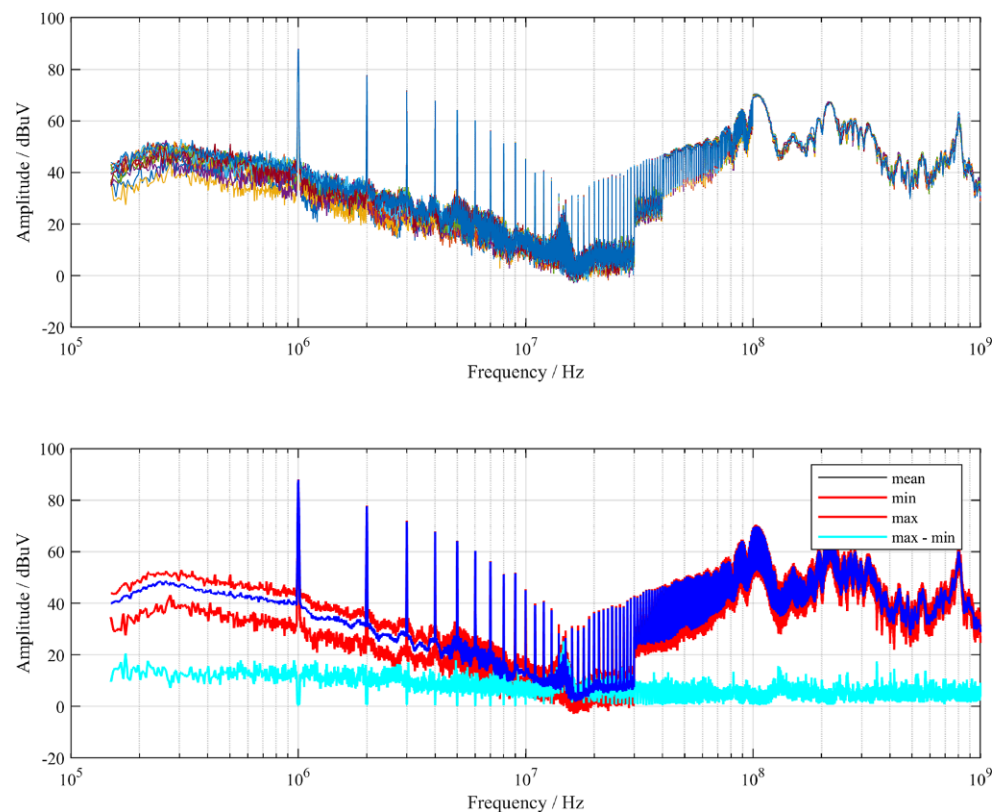
To better analyze the influence of the external decoupling capacitor, we plot the amplitudes of the individual emission peaks, normalized to the value before irradiation, over the course of the dose.

Fig. 8 shows the difference in the amplitudes of the conducted emission with increasing dose. It can be

seen that the fundamental frequency at 1 MHz and the low-order harmonics are little affected by the ionizing radiation. Furthermore, it can be seen that the largest changes in the perturbation amplitudes occur up to about 1 Mrad. Based on this observation, DUT 2 and DUT 3 are subsequently irradiated only up to a dose of 1.5 Mrad.

Fig. 9 shows the difference in the amplitudes of the conducted emission with increasing dose. It can be seen that the fundamental frequency at 1 MHz and

**Fig. 11** Measurements to determine the accuracy of measurements. The upper part of the plot shows all 15 measurements of the spectrum, the lower plot shows the de-logarithmized mean, the minimum and maximum value for each frequency, and the difference between maximum and minimum value. It is remarkable that the uncertainties between the measurements in the actual harmonics are very small, while the measurement uncertainty in the noise is relatively large, although as dwell time the thousandfold of the largest occurring period of the DUT is used



the low-order harmonics are hardly affected by the ionizing radiation. The harmonics above the resonant frequency of the decoupling capacitor are also little affected.

Fig. 10 shows the difference in the amplitudes of the conducted emission with increasing dose. Similar to DUT 2, we show that the low-order harmonics are hardly affected by the ionizing radiation. The harmonics above the resonant frequency of the decoupling capacitor are also little affected.

The observations lead us to conclude that the main influence on the electromagnetic emission is due to the decoupling capacitor. On closer inspection of the area irradiated by the X-ray tube, we realized that in addition to the die in the IC, the decoupling capacitor is also hit by the ionizing radiation. With the help of a fluorescent disk, we were able to determine the entire illumination field of the X-ray tube, as shown in Fig. 4.

Literature shows e.g. [2, 11] and [1] that the multi-layer ceramic capacitors used as decoupling capacitors also show a degradation of performance due to ionizing radiation. This connection explains the strongly changing harmonics around the resonance range of the decoupling capacitor.

#### 4 Uncertainty of Measurement

To determine the validity and repeatability of our measurements, we conduct an investigation into the reproducibility of the individual EMI receiver mea-

surements. For this purpose, we perform 15 consecutive measurements on DUT 2 before irradiation with X-rays. These 15 measurements are then used to generate statistics with an evaluation of the measurement uncertainty.

Fig. 11 shows in the upper part all 15 emission spectra. In the lower part, the arithmetic mean of all measurements, as well as the maximum and the minimum value for each frequency and shown. Additionally, the difference between the maximum and the minimum value for each frequency is illustrated. It is important to note, that the values retrieved by the EMI receiver are in logarithmic scale (dB) and need to be delogarithmized by Eq. (1) in order to be able to do statistics.

$$A_{\text{lin}} = 10^{\frac{A_{\text{dB}}}{20}} \cdot 1 \mu\text{V} \quad (1)$$

In Fig. 11 it can also be seen that the measurement uncertainty in the noise is relatively high, while in the emission peaks the difference between the lowest and highest measured value is less than 1 dB. Therefore, we can say that our measurements of the IC's actual conducted emission and our conclusions are valid.

#### 5 Discussion and outlook

Looking at the individual emission spectra in Figs. 5–7, two general observations emerge. First, the measurements between the emission peaks, the noise floor, differ greatly from measurement to measurement.



Secondly, for all the DUTs, it can be seen that the strongest changes in the noise emission are seen at the resonant frequency of the decoupling capacitor, which suggests that the decoupling capacitor is affected by the ionizing radiation. We can also show, that the on-chip decoupling capacitor is not really influenced by ionizing radiation.

We have shown that the greatest influence of the emission is in the range of the resonant frequency of the external decoupling capacitors, leading to an increase of single harmonics of up to 13 dB. Therefore, in the future we will also look in detail at the radiation-dependent behavior of MLCC capacitors. Thereby we will have a look at the impedance curve at different radiation doses which is important for the improvement of the conducted emissions of an IC.

## 6 Conclusion

In this article, we have analyzed the effect of ionizing radiation on the electromagnetic emission level of ICs. We were able to show that the IC's conducted emission changes significantly in certain frequency ranges. We have shown that this change in noise emission may not come from the IC alone, but from other components relevant for EMC. Thus, it can be seen from our measurement results that the noise emission is significantly influenced by the decoupling capacitor, which in turn has a strong radiation-dependent impedance. We show a considerable annealing effect taking place after 16h, especially lowering the noise floor between the emission peaks. Nevertheless, there is no clear trend due to annealing visible for the generated emission peaks.

**Acknowledgements** Supported by TU Graz Open Access Publishing Fund.

**Funding** Open access funding provided by Graz University of Technology.

**Open Access** This article is licensed under a Creative Commons Attribution 4.0 International License, which permits use, sharing, adaptation, distribution and reproduction in any medium or format, as long as you give appropriate credit to the original author(s) and the source, provide a link to the Creative Commons licence, and indicate if changes were made. The images or other third party material in this article are included in the article's Creative Commons licence, unless indicated otherwise in a credit line to the material. If material is not included in the article's Creative Commons licence and your intended use is not permitted by statutory regulation or exceeds the permitted use, you will need to obtain permission directly from the copyright holder. To view a copy of this licence, visit <http://creativecommons.org/licenses/by/4.0/>.

## References

1. Bastani Y, Cortés-Peña AY, Wilson AD, Gerardin S, Bagatin M, Paccagnella A, Bassiri-Gharb N (2013) Effects of high energy x ray and proton irradiation on lead zirconate titanate thin films' dielectric and piezoelectric response. *Appl Phys Lett*. <https://doi.org/10.1063/1.4805045>
2. Benedetto JM, Moore RA, McLean FB, Brody PS, Dey SK (1990) The effect of ionizing radiation on sol-gel ferroelectric pzt capacitors. *IEEE Trans Nucl Sci* 37(6):1713–1717
3. Benfica J, Green B, Porcher BC, Poehls LB, Vargas F, Medina NH, Added N, de Aguiar VAP, Macchione ELA, Aguirre F, Silveira MAG, Perez M, Sofo HM, Sidelnik I, Blostein J, Lipovetzky J, Bezerra EA (2016) Analysis of sram-based fpga seu sensitivity to combined emi and tid-imprinted effects. *IEEE Trans Nucl Sci* 63(2):1294–1300
4. Benfica J, Vargas F, Soares MF, Schramm D (2020) Conducted emi susceptibility analysis of a cots processor as function of aging. *Microelectronics Reliability* 114:113,884, <https://doi.org/10.1016/j.microrel.2020.113884>
5. Bhat BR, Upadhyaya N, Kulkarni R (2005) Total radiation dose at geostationary orbit. *IEEE Trans Nucl Sci* 52(2):530–534
6. Czepl N, Deutschmann B, Michalowska-Forsyth A (2021) Influence of ionizing radiation on the conducted electromagnetic emission of integrated circuits. *Microelectronics Reliability* 126:114,335, <https://doi.org/10.1016/j.microrel.2021.114335>, <https://www.sciencedirect.com/science/article/pii/S0026271421003012>, proceedings of ESREF 2021, 32nd European Symposium on Reliability of Electron Devices, Failure Physics and Analysis
7. Deutschmann B, Ostermann T (2003) Cmos output drivers with reduced ground bounce and electromagnetic emission. In: ESSCIRC 2004–29th European Solid-State Circuits Conference (IEEE Cat. No.03EX705), IEEE, pp 537–540, <http://doi.org/10.1109/ESSCIRC.2003.1257191>
8. E10 Committee (2018) Guide for ionizing radiation (total dose) effects testing of semiconductor devices. <https://doi.org/10.1520/F1892-12R18>. Accessed November 11 2023
9. Ghfiri C, Boyer A, Bensoussan A, Durier A, Dhia BS (2018) A new methodology for emc prediction of integrated circuits after aging. *IEEE, Transactions on Electromagnetic Compatibility*, pp 1–10 <https://doi.org/10.1109/TEM.2018.2819722>
10. Goerl R, Villa P, Vargas FL, Marcon CA, Medina NH, Added N, Guazzelli MA (2019) Combined ionizing radiation & electromagnetic interference test procedure to achieve reliable integrated circuits. *Microelectronics Reliability* 100–101:113,341, <https://doi.org/10.1016/j.microrel.2019.06.033>
11. Goulding RH, Zinkle SJ, Rasmussen DA, Stoller RE (1996) Transient effects of ionizing and displacive radiation on the dielectric properties of ceramics. *J Appl Phys* 79(6):2920–2933
12. International Electrotechnical Commission (2015-10) Iec 61967 – integrated circuits – measurement of electromagnetic emissions
13. International Electrotechnical Commission (2015-10) Iec 62132 – integrated circuits – measurement of electromagnetic immunity

14. Lara EL, Constante AA, Benfica J, Vargas F, Boyer A, Dhia SB, Gleinser A, Winkler G, Deutschmann B (2021) Impact of place and route strategy on fpga electromagnetic emission. *Microelectronics Reliability* 126:114,333, <https://doi.org/10.1016/j.microrel.2021.114333>
15. Soares MF, Vargas FL, D'Ornelas Benfica J (2021) Conducted emi susceptibility analysis of a cots processor as function of thermal cycling and overvoltage stresses. *Microelectronics Reliability* 126:114,247, <https://doi.org/10.1016/j.microrel.2021.114247>

**Publisher's Note** Springer Nature remains neutral with regard to jurisdictional claims in published maps and institutional affiliations.



**Nikolaus Czepl**, has received the B.Sc. degree and the M.Sc degree in electrical engineering from Graz University of Technology, Graz, Austria, in 2016 and 2018, respectively. He is working towards his PhD degree at Graz University of Technology as university assistant at the Institute of Electronics (IFE). His research interests are robust analog circuit design and combined effects of ionizing radiation and electromagnetic compatibility.



**Nikolaus Juch**, is working on his B.Sc. degree in electrical engineering at Graz University of Technology, Graz, Austria. His research interests are in electromagnetic compatibility and system and chip level.



**Bernd Deutschmann**, received his M.Sc. degree and the Ph.D. degree in telecommunication engineering from the Graz University of Technology/Austria in 1999 and 2002, respectively. After his studies, he worked in the semiconductor industry from 2000 to 2014 on improving the electromagnetic compatibility (EMC) of integrated circuits. In 2014, he returned to academia and moved to Graz University of Technology/Austria as a full professor for "Electronics" and since then heads the Institute of Electronics. His research area is the design of electronic systems and integrated circuits with a special focus on their electromagnetic compatibility. As part of his research activities, he has filed several patents and authored and co-authored numerous papers and technical articles.